

Mixed-Valence Two-Legged MX-Ladder Complex with a Pair of Out-of-Phase Charge-Density Waves

Atsushi Kobayashi* and Hiroshi Kitagawa*

Department of Chemistry, Faculty of Science, Kyushu University, Hakozaki 6-10-1, Fukuoka 821-8581, Japan

Received June 9, 2006; E-mail: akobascc@mbox.nc.kyushu-u.ac.jp; hiroshiscc@mbox.nc.kyushu-u.ac.jp

Mixed-valency is an important requirement in the development of novel electronic materials.¹ Consequently these materials have attracted much attention in the fields of chemistry and physics because of their wide range of interesting physical properties and characteristic electronic system.^{1,2} For a thorough understanding of the complex physics, for example, superconductivity in copper-oxides,³ one needs to develop materials from simple one-dimensional (1D) chains to more complex layered and three-dimensional systems. A typical example of a mixed-valence 1D chain system is the halogen-bridged mixed-valence transition metal complex (the so-called MX chain),⁴ that has drawn much attention because of its unique physical properties such as largest third-order nonlinear optical susceptibility, luminescence with a large Stokes shift,⁶ long-range migration of spin-solitons and polarons along 1D chain,⁷ and so on. Since most of the interesting properties are derived from the mixed-valence strongly covalent 1D chain structure and very weak interchain interaction, crossover from one to two-dimensionality is expected to give a significant effect on the electronic state and physical properties. In fact, the copper-oxide ladder system exhibits interesting properties depending on the number of legs.⁸ In this work, we focused on dimensional crossover and designed a novel two-legged ladder complex, $\{[(\text{dien})\text{Pt}^{\text{IV}}\text{Br}_2\text{-bpy-Pt}^{\text{II}}(\text{dien})]\text{Br}_4\cdot 2\text{H}_2\text{O}\}_\infty$ (dien: diethylenetriamine, bpy: 4,4'-bipyridine) consisting of two parallel MX chains. We propose that it is possible to use a wide range of peripheral tridentate to control the distance between the ladders as well as the bismonodentate ligands forming the rungs to modulate the length of the rungs. These should provide continuous tuning of the important parameters involved in the electronic processes responsible for the intervalence charge transfer.

The ladder structure of $\{[(\text{dien})\text{Pt}^{\text{IV}}\text{Br}_2\text{-bpy-Pt}^{\text{II}}(\text{dien})]\text{Br}_4\cdot 2\text{H}_2\text{O}\}_\infty$ is shown in Figure 1.⁹ The building units consisting of two Pt-dien linked by a bpy is clearly identified and the ladder structure is constructed by stacks of these binuclear units with bridging bromine atoms on one of the Pt. Since the bridging bromide ions deviate from the midpoint between adjacent platinum ions within each leg ($\text{Pt}^{\text{II}}\cdots\text{Br}$ (l_1): 2.9652(13) Å, $\text{Pt}^{\text{IV}}\text{-Br}$ (l_2): 2.5041(13) Å), the electronic structure in each Pt-Br leg is attributable to the charge-density-wave (CDW) state ($\cdots\text{Pt}^{\text{II}}\cdots\text{Br}\text{-Pt}^{\text{IV}}\text{-Br}\cdots\text{Pt}^{\text{II}}\cdots\text{Br}\text{-Pt}^{\text{IV}}\text{-Br}\cdots$). A long overtone progression of $\nu(\text{Pt-Br})$ mode was observed (see Figure S1), which is another evidence for the CDW state on the ladder, and it is forbidden in the single-valence state of $\text{-Pt}^{\text{III}}\text{-Br}\text{-Pt}^{\text{III}}\text{-Br-}$, while allowed in the CDW state.^{4g,4h} The energy of the $\nu(\text{Pt-Br})$ mode at 172 cm^{-1} is higher by about 16 cm^{-1} than that of $[\text{Pt}(\text{chxn})_2\text{Br}]_2$ where the $\text{Pt}^{\text{IV}}\text{-Br}$ distance 2.498(7) Å is almost the same as that of the ladder complex,^{4e} indicating that the MX-ladder lattice is more rigid than the MX-chain one.

Because of the absence of Pt atoms on crystallographic special positions and the lack of any symmetry relating Pt^{II} to Pt^{IV} , all the bridging bromine atoms are well ordered. Judging from arrange-

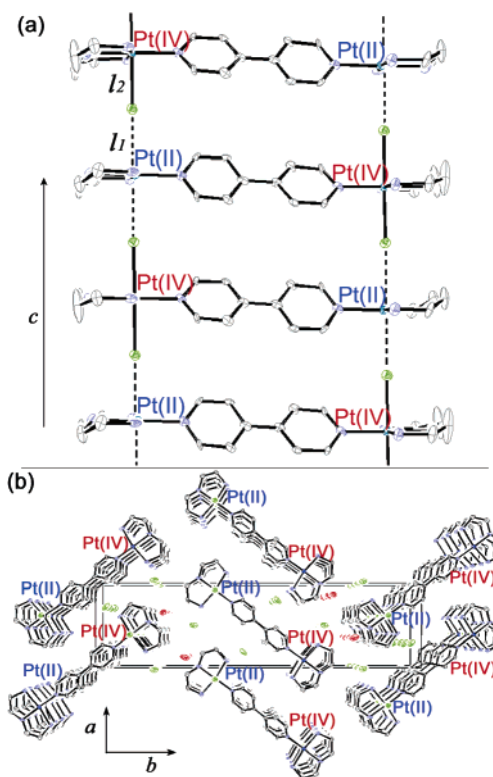


Figure 1. (a) Ladder structures of $\{[(\text{dien})\text{Pt}^{\text{IV}}\text{Br}_2\text{-bpy-Pt}^{\text{II}}(\text{dien})]\text{Br}_4\cdot 2\text{H}_2\text{O}\}_\infty$. The valence states of Pt ions are displayed. Panel b shows a perspective view of unit cell along the *c*-axis. The valence states of Pt ions on the same *ab* plane are displayed.

ments of the bridging Br^- deviations, a pair of out-of-phase CDWs is formed in the ladder as displayed in Figure 1a. As is clearly seen in Figure 1b, the arrangement of a pair of CDWs is also ordered between neighboring ladders. This is the first example of a three-dimensionally ordered CDW in the crystal among more than 200 salts displaying CDW-type MX chains. In general, the MX chains have no interchain ordering in CDWs because of a weak interaction between the chains, and a few display two-dimensionally ordered CDWs,¹⁰ except for a few complexes with bent chain structure.¹¹ In case of the first reported two-legged ladder complex based on the MX chain $\{[(\text{en})\text{Pt}^{\text{IV}}\text{Br}_2\text{-bpym-(Pt}^{\text{II}}\text{en)}](\text{ClO}_4)_4\}_\infty$ (en: ethylenediamine, bpym: 2,2'-bipyrimidine) which has shorter distance between the two MX legs on the ladder (ca. 5.5 Å), that is the rung length, than our complex, it remains unclear whether this complex has an intraladder ordering of CDWs or not, owing to an incomplete crystal structure.¹² As a result of a relatively long bpy ligand connecting the two MX-legs, the rung length (11.17 Å) is longer than the distances between nearest (8.77 Å) and second nearest ladder legs (9.25 Å). These intra- and interladder MX-leg distances are longer than the interchain distance in $[\text{Pt}(\text{chxn})_2\text{Br}]_2$ -

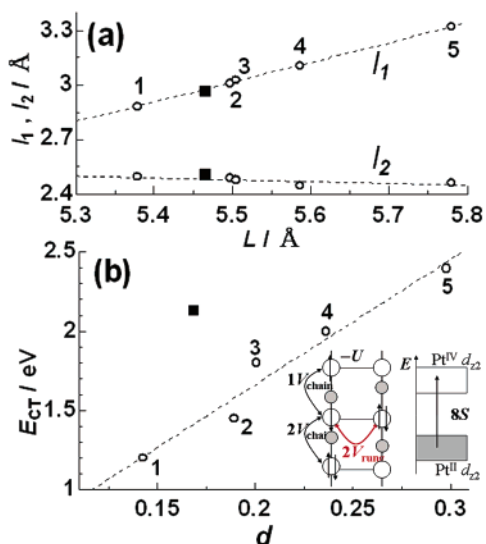


Figure 2. (a) Correlation between the Pt–Pt (L) and Pt–Br (l_1 and l_2) distances; (b) the CT excitation energies (E_{CT}) plotted against the distortion parameter d ($= 2(l_1 - l_2)/L$). Inset shows the parameters contributing to E_{CT} . $\{[(\text{dien})\text{Pt}^{\text{IV}}\text{Br}_2\text{-bpy-Pt}^{\text{II}}(\text{dien})]\text{Br}_4 \cdot 2\text{H}_2\text{O}\}_\infty$ is plotted as closed square. PtBr chains are plotted as open circles. Data shown for (1) $[\text{Pt}(\text{chxn})_2\text{Br}]\text{-Br}_2$, (2) $[\text{Pt}(\text{en})_2\text{Br}](\text{ClO}_4)_2$ (3) $[\text{Pt}(\text{NH}_3)_4\text{Br}](\text{HSO}_4)_2$, (4) $[\text{Pt}(\text{etn})_4\text{Br}]\text{-Br}_2$, (5) $[\text{Pt}(\text{chxn})_2\text{Br}](\text{ClO}_4)_2$ (see ref 4e). The dotted lines are drawn for a guide.

Br_2 (chxn: 1*R*,2*R*-diaminocyclohexane), where the CDWs are two-dimensionally ordered in the *ab*-plane with a distance of 7.028 Å (*ll* *b*).^{4e,10a} Despite the long rung, the pair of CDWs on the ladder is ordered in out-of-phase, implying that there exists a charge-transfer interaction between Pt^{II} and Pt^{IV} sites through the rung. As for the interladder CDWs' ordering, the Madelung potential may also be playing an important role.

Figure 2a shows the Pt^{II}–Br (l_1) and Pt^{IV}–Br (l_2) distances as a function of the Pt–Pt distance ($L = l_1 + l_2$) for several PtBr-chain complexes and $\{[(\text{dien})\text{Pt}^{\text{IV}}\text{Br}_2\text{-bpy-Pt}^{\text{II}}(\text{dien})]\text{Br}_4 \cdot 2\text{H}_2\text{O}\}_\infty$. Figure 2b displays the correlation between the distortion parameter d defined by $2(l_1 - l_2)/L$ and the intervalence charge-transfer excitation energy (E_{CT}) estimated from the diffuse reflectance spectrum (see Figure S2, Supporting Information). It is well-known that the shorter L is the longer l_2 and shorter l_1 owing to the larger overlap integral between Pt and Br, resulting in the lower E_{CT} .^{4d} As is clearly seen in Figure 2a, the l_1 and l_2 distances of the MX-ladder $\{[(\text{dien})\text{Pt}^{\text{IV}}\text{Br}_2\text{-bpy-Pt}^{\text{II}}(\text{dien})]\text{Br}_4 \cdot 2\text{H}_2\text{O}\}_\infty$ fall on the dotted lines which shows good correlations between the Pt–Pt and Pt–Br distances in MX chains. Nevertheless, the E_{CT} of $\{[(\text{dien})\text{Pt}^{\text{IV}}\text{Br}_2\text{-bpy-Pt}^{\text{II}}(\text{dien})]\text{Br}_4 \cdot 2\text{H}_2\text{O}\}_\infty$ shows significant deviation, indicating a large difference in electronic state between the ladder and chain. According to the extended Peierls–Hubbard model,^{4,13} the E_{CT} in the ladder with a pair of out-of-phase CDWs can be given by

$$E_{CT} = 8S + 2V_{\text{rung}} + 3V_{\text{chain}} - U$$

where S is the electron–lattice interaction, U is the on-site Coulomb repulsion, V_{rung} and V_{chain} are the intersite Coulomb repulsion along the rung and chain, respectively (see Figure 2b inset and Figures S3 and S4). For the MX-chain with CDW, on the other hand, $E_{CT} = 8S + 3V_{\text{chain}} - U$, because $V_{\text{rung}} = 0$, resulting that the E_{CT} is higher in the MX-ladder than in the MX-chain.

In summary, we have synthesized a novel two-legged MX-ladder $\{[(\text{dien})\text{Pt}^{\text{IV}}\text{Br}_2\text{-bpy-Pt}^{\text{II}}(\text{dien})]\text{Br}_4 \cdot 2\text{H}_2\text{O}\}_\infty$, having a pair of out-

of-phase CDWs within each ladder. These pairs of CDWs are ordered from ladder to ladder, which is the first example of a three-dimensionally ordered CDW state observed for the MX-chain complexes. The CT excitation energy in the MX ladder was found to be significantly higher than that in the MX-chain, which is due to the intersite Coulomb repulsion V_{rung} along the rung. Further work to look for any interference effect due to two concerted electron transfer or spin exchange interaction along the two legs of a ladder is in progress.

Acknowledgment. This work was partly supported by a Grant-in-Aid for Scientific Research on Priority Areas (Chemistry of Coordination Space, No. 16074212) and the Joint Project for Chemical Synthesis Core Research Institutions, from the Ministry of Education, Culture, Sports, Science and Technology, Japan, a Grant-in-Aid for Scientific Researches (B) No. 14340215 and No. 16350033 from the Japan Society for the Promotion of Science, and by the Kurata Memorial Hitachi Science and Technology Foundation.

Supporting Information Available: X-ray crystallographic files in CIF format, Raman and diffuse reflectance spectrum of $\{[(\text{dien})\text{Pt}^{\text{IV}}\text{Br}_2\text{-bpy-Pt}^{\text{II}}(\text{dien})]\text{Br}_4 \cdot 2\text{H}_2\text{O}\}_\infty$. This material is available free of charge via the Internet at <http://pubs.acs.org>.

References

- (1) *Mixed-valence compounds: Theory and Applications in Chemistry, Physics, Geology and Biology*; Brown, D. B. Ed., Kluwer: Boston, MA, 1980.
- (2) (a) Demadis, K. D.; Hartshorn, C. M.; Meyer, T. *J. Chem. Rev.* **2001**, *101*, 2655–2685. (b) Chang, C. C.; Pfenning, B.; Bocarsly, A. B. *Coord. Chem. Rev.* **2000**, *208*, 33–45. (c) N. Kojima, N. Matsushita, *Coord. Chem. Rev.* **2000**, *198*, 251–263.
- (3) (a) Bednorz, J. G.; Mueller, K. A. *Z. Phys.* **1986**, *64*, 189. (b) Wu, M. K.; Ashburn, J. R.; Torng, C. J.; Hor, P. H.; Meng, R. L.; Gao, L.; Huang, Z. J.; Wanag, Y. Q.; Chu, C. W. *Phys. Rev. Lett.* **1987**, *58*, 908–910.
- (4) (a) Matsumoto, N.; Yamashita, M.; Kida, S. *Bull. Chem. Soc. Jpn.* **1978**, *51*, 2334–2337. (b) Nasu, K. *J. Phys. Soc. Jpn.* **1983**, *52*, 3865–3873. (c) Nasu, K. *J. Phys. Soc. Jpn.* **1984**, *53*, 302–311. (d) Okamoto, H.; Mitani, T.; Toriumi, K.; Yamashita, M. *Mater. Sci. Eng., B* **1992**, *13*, L9–L14. (e) Scott, B.; Love, S. P.; Kanner, G. S.; Johnson, S. R.; Wilkerson, M. P.; Berkey, M.; Swanson, B. I.; Sexena, A.; Huang, X. Z.; Bishop, A. R. *J. Mol. Struct.* **1995**, *356*, 207–229. (f) Yamashita, M.; Ishii, T.; Matsuzaka, H.; Manabe, T.; Kawashima, T.; Okamoto, H.; Kitagawa, H.; Mitani, T.; Marumoto, K.; Kuroda, S. *Inorg. Chem.* **1999**, *38*, 5124–5130. (g) Okamoto, H.; Toriumi, K.; Okaniwa, K.; Mitani, T.; Yamashita, M. *Synth. Met.* **1991**, *41–43*, 2791–2794. (h) Manabe, T.; Kawashima, T.; Yamashita, M.; Kaga, Y.; Okamoto, H.; Kitagawa, H.; Mitani, T. *Synth. Met.* **1999**, *102*, 1779–1780.
- (5) Kishida, H.; Matsuzaki, H.; Okamoto, H.; Manabe, T.; Yamashita, M.; Taguchi, Y.; Tokura, Y. *Nature*, **2000**, *405*, 929–932.
- (6) Tanino, H.; Kobayashi, K. *J. Phys. Soc. Jpn.* **1983**, *52*, 1446–1456.
- (7) (a) Kimura, N.; Ishimaru, S.; Ikeda, R.; Yamashita, M. *J. Chem. Soc., Faraday Trans.* **1998**, *94*, 3659–3663. (b) Okamoto, H.; Mitani, T.; Toriumi, K.; Yamashita, M. *Phys. Rev. Lett.* **1992**, *69*, 2248–2251.
- (8) (a) Hiroi, Z.; Takano, M. *Nature*, **1995**, *377*, 41–43. (b) Azuma, M.; Hiroi, Z.; Takano, M.; Ishida, K.; Kitaoka, Y. *Phys. Rev. Lett.* **1994**, *73*, 3463–3466. (c) Dagotto, E.; Rice, T. M. *Science* **1996**, *271*, 618–623.
- (9) See Supporting Information for details of the synthesis and X-ray crystal structural analysis of $\{[(\text{dien})\text{Pt}^{\text{IV}}\text{Br}_2\text{-bpy-Pt}^{\text{II}}(\text{dien})]\text{Br}_4 \cdot 2\text{H}_2\text{O}\}_\infty$.
- (10) (a) Iwasa, K.; Wakabayashi, N.; Sakai, M.; Kuroda, N.; Nishina, Y. *J. Phys. Soc. Jpn.* **1992**, *61*, 3625–3630; (b) Wakabayashi, Y.; Wakabayashi, N.; Kuroda, N.; Nishida, M.; Matsushita, N. *J. Phys. Soc. Jpn.* **1998**, *67*, 186–191; (c) Wakabayashi, Y.; Wakabayashi, N.; Yamashita, M.; Manabe, T.; Matsushita, N. *J. Phys. Soc. Jpn.* **1999**, *68*, 3948–3952.
- (11) (a) Clark, R. J. H.; Kurmoo, M.; Galas, A. M. R.; Hursthouse, M. B. *J. Chem. Soc., Dalton Trans.* **1983**, 1583–1586. (b) Fanizzi, F. P.; Natile, G.; Lanfranchi, M.; Tiripicchio, A.; Clark, R. J. H.; Kurmoo, M. *J. Chem. Soc., Dalton Trans.* **1986**, 273–278. (c) Badar-Ud-Din; Bailar, J. C., Jr. *J. Inorg. Nucl. Chem.* **1961**, *22*, 242–245.
- (12) Yamashita, M.; Kawakami, D.; Matsunaga, S.; Takaishi, S.; Miyasaka, H.; Sugiura, K.; Matsuzaki, H.; Kishida, H.; Okamoto, H.; Tanaka, H.; Kuroda, S. The Autumn Meeting of the Physical Society of Japan, 13pWF-10, Aomori, 2004.
- (13) K. Iwano. The Annual Meeting of the Physical Society of Japan, 27pYK-5, Noda, 2005.

JA064082O